JOURNAL OF Applied Polymer SCIENCE

Melt Processing and Characterization of Polyvinyl Alcohol and Polyhydroxyalkanoate Multilayer Films

Christopher Thellen, Sarah Cheney, Jo Ann Ratto
Combat Feeding Directorate, U.S. Army Natick Soldier Research Development and Engineering Center, Natick, Massachusetts 01760

Correspondence to: C. Thellen (E-mail: christopher.t.thellen.civ@mail.mil)

ABSTRACT: Multilayer films for food packaging applications composed of polyvinyl alcohol (PVOH) as the core layer and polyhydroxyalkanoate (PHA) as the outer skin layers were produced by the co-extrusion process. Rheological properties of PVOH and PHA were performed and analyzed before co-extruding into a cast film. Analysis of the rheological data indicated the processing temperatures and grades of the PVOH and PHA polymers that would produce similar viscosity and melt flow properties. To improve adhesion of the layers, PHA was grafted with maleic anhydride using a dicumyl peroxide initiator to provide a tie layer material, which improved the peel strength of the PHA and PVOH layers by over 2×. Oxygen transmission rate (OTR) testing showed that the multilayer sample provided an OTR of 27 cc/m^2-day at 0% relative humidity (RH) and rates of 41 and 52 cc/m^2-day at relative humidity values of 60% and 90% RH, respectively. This indicates significant barrier performance enhancement over monolayer PVOH that provided an OTR of 60 cc/m^2-day at 0% RH and 999 cc/m^2-day at 60% RH. Biodegradation testing of the films in the marine environment showed that both the unmodified and maleated PHA polymers displayed high levels of mineralization, whereas the PVOH material did not. © 2012 Wiley Periodicals, Inc. J. Appl. Polym. Sci. 000: 000–000, 2012

KEYWORDS: polyvinyl alcohol; polyhydroxyalkanoate; barrier; coextrusion; multilayer films; permeation

Received 21 December 2011; accepted 30 March 2012; published online
DOI: 10.1002/app.37850

INTRODUCTION

Representing a $38 billion global market, the flexible packaging industry is growing rapidly. With the demand for flexible packaging growing at an average rate of 3.5% each year, flexible materials need to meet and exceed the high expectations of consumers and the stressors of the supply chain.[1] Increased competition between suppliers, along with government regulations, have resulted in innovations in films that enhance product and package performance, as well as address worldwide concerns with packaging waste.[1] Concerns over the persistence of plastics in the environment, shortage of landfill space, emissions during incineration, and a negative impact on wildlife through ingestion and entrapment in the marine environment have increased research and development efforts on green bio-based alternatives and/or biodegradable polymers. However, improvements in biodegradability typically come at the expense of performance and processability, and trade-offs often need to be made in achieving performance while maintaining biodegradation.[2] Sustainability is currently a dynamic force for industry to use green, bio-based, compostable materials. The use of biodegradable polymers that are disposed of through composting can reduce the amount of solid waste generated in most areas of the world. This alone is a significant reason to use biodegradable polymers; however, there needs to be a balance with price, performance, properties, and manufacturing methods used to create these polymers.[3] Among biodegradable materials, three families are usually considered.[4] The first being polymers directly extracted from biomass such as polysaccharides, starch, chitosan, and cellulose as well as proteins such as gluten, soy protein, and zein. A second family comprises petroleum-based monomers or biomass-derived monomers, but uses classical chemical synthetic routes to obtain the final biodegradable material; this is the case for poly(e-caprolactones) (PCL), polyvinyl alcohol (PVOH), and polylactic acid (PLA). The third family comprises polymers produced by natural or genetically modified microorganisms instead of plants. Examples of these include polyhydroxyalkanoates (PHAs) and polypeptides.[5]

PVOH is considered to be inherently biodegradable and has been the subject of extensive technological advances over the past few years.[6] It has been demonstrated that PVOH can be

efficiently degraded only in the presence of selected microorganisms whose occurrence in natural environments may be relatively uncommon. This information is in keeping with the limited biodegradation of many PVOH-based items in natural solid matrices such as soil and compost, as well as in aqueous media lacking specific PVOH-degrading microorganisms.[7] It was first synthesized in 1924 by Herman and Haehnel by the hydrolysis of polyvinyl acetate and its major initial use was for textile sizing.[8,9] PVOH has traditionally been useable or processable only in the form of aqueous solutions or films cast from these, rather than as a thermoplastic. However, recent breakthrough proprietary technologies have now led to the development and commercial introduction of a family of PVOH-based thermoplastics, containing no toxic additives and with good melt processability, outstanding properties and versatility, at similar cost to most other biodegradable plastics. These PVOH-based materials represent a viable biodegradable and compostable alternative to present nondegradable materials for many applications.[10] Recently developed, proprietary formulating and processing technologies represent a highly significant technological advance in allowing PVOH grades from partially to fully hydrolyzed, and including the highest commercially available molecular weights, to be processed as thermoplastics while still retaining a wide range of desirable property combinations.[11–13] In regards to gas barrier properties, PVOH-based materials have very low permeability (i.e., high barrier characteristics) toward oxygen, carbon dioxide, and nitrogen, often lower than ethylene co-vinyl alcohol (EVOH) co-polymers, and much lower permeability as compared with other traditional polyolefins. However, they are quite permeable toward water vapor, which acts as a plasticizer and compromises their excellent oxygen barrier properties. This behavior pattern is in contrast to that of polyethylene which is relatively permeable toward oxygen, nitrogen, and carbon dioxide but is a high water vapor barrier material.

PHAs are a family of biopolyesters, which have thermoplastic properties that can be tailored to specific applications by varying their chemical structure.[14] The physical properties of poly 3-hydroxybutyrate (P3HB) copolymers, a member of the PHA family, are often compared with isotactic polypropylene (PP). These physical properties vary according to the content of 3-hydroxybutyrate in the copolymer as crystallinity and density increase with increasing 3-hydroxybutyrate content. In regards to permeation of gases, higher 3-hydroxybutyrate contents typically decrease oxygen permeation rates to levels that are superior to those of uncoated polyolefins (269–410 cc mil/m^2-day) and water vapor permeation rates (WVPRs) of 161–217 g mil/m^2-day.[15] Most PHA polymers have been shown to be highly biodegradable in numerous environments such as soil, fresh water, marine water, compost, and activated sludge.[16–22] There are numerous methods from the American Society for Testing and Materials (ASTM) and International Standards for measuring biodegradability of polymers. These standards describe the degree of biodegradation and the time frame in which it must occur.[3] Because of the film-forming capability of PHA resins, they have been marketed as biodegradable and environmentally benign, targeting packaging materials in the agriculture, military, and medical fields.[23] The U.S. Navy has been targeting marine biodegradable polymers to help reduce the amount of solid waste on board ship. The U.S. Navy in conjunction with the U.S. Army has explored biodegradable polymers and their biodegradation rates. PHA polymers are unique in that they are truly biodegradable in the marine environment with mineralization rates meeting the ASTM 7081 specification within as little as a month's time.[24] Therefore, biodegradation measurements of PHA-based polymer and the multilayer films in this study will help to enable the application of this polymer family and use its marine biodegradable nature.

Multilayer films produced through the co-extrusion and lamination processes are often used to provide enhanced barrier properties to gases such as oxygen, nitrogen, and water vapor.[25] The gas transmission rate at steady state through a given polymer layer is inversely proportional to the thickness of the layer. The theoretical transmission rate of a multilayer film structure may be estimated by summing the resistances of each layer.[26] One of the most important problems facing multilayer films is the adhesion of layers made of various materials to one another. When working with incompatible materials, a tie layer will most likely be required for adhesion purposes. Tie layers act as an adhesive, and most have been developed for use with polyolefin resins. Numerous specialty tie resins are available today including ethylene acrylic acid-based materials and maleic anhydride graft resins.[27]

This research focuses on the processing and characterization of multilayer film formulations of biodegradable PHA and PVOH with emphasis on improving peel strength between the layers and taking advantage of the high oxygen barrier/solubility properties of PVOH as well as the biodegradable/water-vapor barrier properties of PHA. The multilayer films incorporate PHA as the skin layers and various grades of PVOH as the core layer. The grades of PVOH vary in levels of hydrolysis, molecular weight, and crystallinity. Typical PHA materials demonstrate WVPRs which are slightly higher than polyethylene (10–15 g mil/m^2-day), but significantly lower than biodegradable polymers such as PLA and PCL (3400–3600 g mil/m^2-day).[28] The PHA layer is used to protect the hydrophilic PVOH layer from atmospheric moisture, thereby providing an improved barrier structure under conditions of elevated relative humidity.

EXPERIMENTAL

Materials

The PVOH resins that were examined in this study were of varying degrees of hydrolysis and plasticizer content. PVOH H-80 (99% hydrolyzed) and PVOH W-60 (96% hydrolyzed) were supplied by Stanelco in both film and resin form. Aqua-Sol 116 PVOH (88–90% hydrolyzed) was provided by A. Schulman in resin form and POVAL CP-1220T10 PVOH (73% hydrolyzed) was supplied by Kuraray America. The POVAL PVOH contained 20% polyethylene glycol (PEG) plasticizer and 10% talc. PEG is not considered to be biodegradable and future work involving biodegradable plasticizers as a PEG alternative would aid in meeting biodegradable standards such as ASTM D7081 and ASTM D6400. The Aqua-Sol PVOH resin is also plasticized with a biodegradable plasticizer system, but no further information was disclosed from the supplier.

PHA materials were supplied by Telles, a former joint-venture between Metabolix and Archer Daniels Midland Company. Materials supplied included their paper coating grade resin (Mirel^{TM} P2001) and a film grade (Mirel^{TM} P5001). All grades are co-polymer forms of P3HB-4HB with a proprietary nucleating agent. PHA grafting reactions were conducted using 99% Maleic anhydride (Avocado Research Chemicals) and 98% Dicumyl peroxide (Sigma-Aldrich Company).

Co-Extrusion

Three-layer melt extruded films were processed at the laboratory-scale using a Dr. Collin GmbH Teach-Line^{TM} multilayer system with three 20-mm screw extruders having a 25 : 1 *L*/*D* ratio. Feed-block technology was used to assemble the extrudate layers into the three-layer film by way of a 120 mm adjustable thickness slot die and temperature regulated cast film chill rolls, which were maintained at a roll temperature of 60°C to accelerate crystallization of the PHA films and limit sticking onto the rolls.

Production of Maleic Anhydride-Grafted PHA

Reactive extrusion processing was used to graft maleic anhydride onto the PHA polymer by way of a DSM conical twin-screw recirculating microcompounding unit. The reaction was carried out by premelting the PHA resin in the barrel of the microcompounder at barrel temperatures of 180°C and a screw speed of 120 rpm for 1 min. This produced a PHA melt temperature of 172°C. Maleic anhydride was gently warmed to a liquid state at 70°C in a glass beaker on a hot-plate. Dicumyl peroxide was then added to the liquid maleic anhydride at a ratio of 1 : 8 and stirred until the peroxide was entirely dissolved in the maleic anhydride. This solution was injected into the microcompounder, containing the molten PHA, so that the composition of the PHA/maleic anhydride/dicumyl peroxide mixture was 95.5 : 4 : 0.5, respectively. This was mixed for a period of 3 min and extruded out of the compounder in strand form and pelletized into granules. These granules were added back into the microcompounder and mixed for an additional minute under the same conditions. Dicumyl peroxide was again added to the mixture at 0.5% by weight and the entire batch was mixed for an additional 3 min before being extruded and pelletized once more. The compounding time for the reaction was determined by calculating the time needed to run the reaction to an extent of 97% based on the half-life of the dicumyl peroxide at the processing temperature of 172°C.[29] The final pellets were dried in a vacuum oven overnight at 80°C. To purify the PHA and remove any residual maleic anhydride from the pellets, the pellets were dissolved in chloroform at 40°C at a loading of 5% by weight. Ethanol was slowly added at a ratio of 5 : 1 to precipitate out the polymer, whereas residual maleic anhydride was left in solution. Distilled water was used to wash the precipitate after being filtered. The precipitate was allowed to dry under vacuum at 60°C for 4 h to remove water and any remaining solvent.

The lamination of multilayer films using the maleic anhydride grafted PHB polymer was accomplished using a heated Carver press. Control multilayer samples were made by pressing a 50 μ PVOH film with a 50 μ PHB film at 174°C for 10 s at 4 bar (50 psig). Multilayer film samples containing the PHB-*g*-MA were made in the same manor, substituting the PHB film with the PHB-*g*-MA film.

Characterization

Rheology. Melt rheology was measured using a Dynisco LCR 7001 capillary rheometer. The barrel length of the rheometer was 200 mm and the die used was a CX300-33, with a diameter of 0.762 mm and length of 25.10 mm giving and *L*/*D* ratio of 33 : 1. Testing temperatures were based on the extrusion melt processing window for each polymer. When testing, each specimen was run at eight different shear rates of 5000, 2000, 1000, 500, 250, 100, 50, and 20 s^{-1}.

Barrier Properties. Oxygen barrier properties of the film samples were measured using an Illinois Instruments 8001 Permeation Analyzer (Serial No. 80-09611007) following ASTM D3985. Samples were kept in a conditioning chamber for 1-week before testing at the relative humidity conditions used during the tests. Two 50 cm^2 specimens were tested for each sample at 0%, 60%, and 90% RH. All specimens were tested at a temperature of 23°C and experiments ran until an equilibrium permeation rate had been reached using the instruments auto-stop feature which stopped the experiment when three consecutive readings fell within 1% of each other. Readings were taken every 60 min.

Mechanical Properties. Tensile testing was conducted on an Instron® 4400R tensile testing machine with a 50 kN load cell following ASTM Standard D882. Samples were kept at room temperature and 50% RH for 1 week before testing. Layer to layer adhesion (peel strength) was also measured using this Instron machine with 12.7 mm (0.5 in) wide samples. The multilayered specimens were initially delaminated by hand using a razor blade. Opposing layers of the sample were then inserted into the Instron grip and tested at a gauge length of 50.8 mm and a crosshead speed of 50 mm/min. For each sample set, five specimens were tested with the average and standard deviation recorded.

Thermal Analysis. Thermal analysis of the samples was conducted through differential scanning calorimetry (DSC). DSC was performed on a TA Instruments Q100 DSC. The PVOH samples were heated from −50°C to 240°C at 10°C per min, held isothermal for 2 min at 240°C, quench cooled to −50°C, and then heated once again to 240°C at a rate of 10°C per min. The first heating scan was used to determine sample crystallinity of the films as received from the extrusion trials. A TA Instruments Q800 model dynamic mechanical analysis (DMA) in multistrain mode was also used to investigate the glass transition temperature of the films. Samples were tested by first equilibrating at −70°C and then heating at 4°C/min to 80°C at a frequency of 4 Hz and a preload force of 0.01 N. Alpha glass transition temperatures were measured by determining the peak maximum of the loss modulus curve in each DMA scan. Samples were initially scanned in their original state and a second set of samples were tested after being conditioned for 5 days at 50°C in a laboratory oven. This was done to condition all film samples at the same environmental conditions to achieve similar moisture content for DMA testing. Moisture analysis was done on a Mitsubishi Karl Fischer Moisture Meter (Model CA-100

with VA-100 vaporizer) at a test temperature of 140°C before the titration process.

Grafting Characterization. The success of grafting maleic anhydride onto the PHA polymer was determined using Fourier transform infrared spectrometry (FTIR) and Carbon (^{13}C) nuclear magnetic resonance (NMR) spectroscopy. FTIR studies were conducted on a model 6700 Thermo Nicolet system with Omnic 8 software. The samples were analyzed on a Thermo Scientific Smart iTR attenuated total reflectance single bounce attachment equipped with a diamond crystal. ^{13}C-NMR spectra were obtained on the samples in solution state using a Bruker Biospin 400 MHz Avance spectrometer. Proton-decoupled carbon-13 spectra were acquired using a power-gated decoupling pulse sequence, with a 30° flip angle and rotation speed of 20 Hz. Raw data were acquired as free induction decays and processed with a line broadening of 1.0 Hz. ^{13}C-NMR Spectra were referenced to the chloroform peak at 77.7 ppm.

Biodegradation in the Marine Environment. Biodegradation in the marine environment was examined through respirometry experimentation according to ASTM D6691 "Standard Test Method for Determining Aerobic Biodegradation of Plastics Materials in the Marine Environment by a Defined Microbial Consortium or Natural Sea Water Inoculum," where natural seawater collected from Hampton Beach, NH in July 2010 was used as the testing medium. Columbus Instruments respirometers were used to measure carbon dioxide evolution of each sample as a function of time along with Kraft paper as a positive control and natural sea water as a negative baseline control.

RESULTS AND DISCUSSION

Co-Extrusion

In co-extrusion of polymers, the matching of polymer viscosity at the processing temperature is critical because melt viscosity mismatch can result in interfacial instabilities, as well as polymer encapsulation.[30] To determine the proper processing temperatures for the selected PHA and PVOH polymers, shear rate-viscosity curves were generated using the capillary rheometer. Figure 1 illustrates shear rate versus viscosity curves for two commercial grades of PHA (Mirel^{TM} P2001 and Mirel^{TM} P5001), and Figure 2 illustrates curves with two melt-extrusion grades of PVOH (W-60 and POVAL CP-1220T10) at temperatures that were considered for extrusion processing.

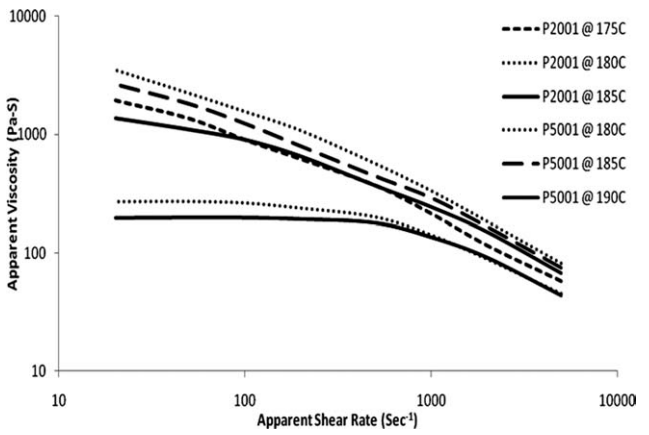

Figure 1. Apparent viscosity of PHA polymers at various processing temperatures.

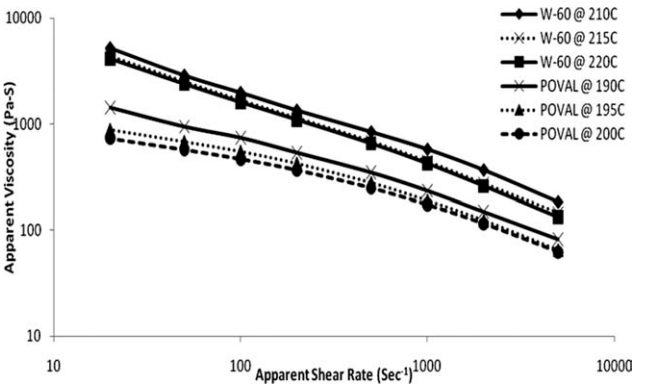

Figure 2. Apparent viscosity of PVOH polymers at various processing temperatures.

From these results, the optimal polymer viscosity matching under typical extrusion shear rates (100–1000 s^{-1}) was achieved with the POVAL PVOH at a melt temperature of 190°C and with the Mirel^{TM} P2001 PHA at a melt temperature of 180°C. Therefore, the POVAL PVOH and the Mirel^{TM} P2001 PHA materials were selected for the co-extrusion process based on this rheological data. Film instabilities during the processing may be eliminated by altering the melt temperature or shear rate of these polymers to more closely match viscosity values.

The co-extrusion system was set-up so that one extruder produced the core POVAL PVOH layer, whereas a second extruder produced the Mirel^{TM} P2001 skin layers by using a feed block to form and combine each layer in the A-B-A type three-layer structure. A 150-mm adjustable thickness sheet die was used to extrude the polymers onto a set of steel rolls set at a temperature of 60°C to maximize PHA polymer crystallinity. Initial DSC analysis indicated that the optimum temperature for crystallization of this grade of PHA was 60°C. The steel rolls were set to this temperature so that continued crystallization during processing would provide enhanced film barrier properties. Before extrusion processing, PHA and PVOH resins were dried overnight in a desiccating dryer at 90°C to reach moisture contents of <0.1%. Optimized extrusion conditions are listed in Table I for this co-extrusion trial.

The film produced through the co-extrusion cast film die appeared to have no layer-to-layer melt disturbances such as melt-fracture (sharkskin), nonhomogeneous melting, or interfacial instabilities (waves, zig-zag, arrow heads, chevrons, etc.).[31] This high quality film did not indicate any problems with viscosity or melt velocity differences between the flowing polymer layers.[26] However, once the film was collected onto a roll, it became apparent that delamination was beginning to occur between the polymer layers (PHA and PVOH) in the multilayer film. Peel strength testing confirmed that the peel strength between the PHA and the PVOH layers in the film was only 0.004 N/mm.

Table I. Co-Extrusion Processing Conditions

Polymer	Screw speed (rpm)	Zone 1 (°C)	Zone 2 (°C)	Zone 3 (°C)	Zone 4 (°C)	Die (°C)	Melt temperature (°C)
POVAL PVOH	35	180	185	190	200	195	189
PHA P2001	65	180	185	185	190	195	181

Barrier properties of the film sample were analyzed to determine the affect of the PHA skin layers on the PVOH core layer. Table II lists the measured barrier properties for each material component along with the multilayer film and the theoretical transmission rate, which was calculated by the summation of resistance model discussed earlier.

Clearly, the barrier properties of the PVOH were highly susceptible to relative humidity, which is expected because PVOH is water soluble. The barrier properties of the PHA were also only slightly affected by relative humidity. Barrier results indicated that the oxygen transmission rate (OTR) of the PVOH core increased from 60 to 999 cc/m^2-day in a 4.9-mil thick film when the RH of the testing environment was raised from 0 to 60% RH. Test failure occurred when the RH of the test was raised to 90% as the OTR exceeded the upper limit of the sensor which is 432,000 cc/m^2-day. This is in sharp contrast to the 5.1-mil thick PHA film which exhibited an increase in OTR of 211 to only 250 cc/m^2-day (18% increase) after increasing the RH of the test from 0 to 90% RH. Under the same conditions, the multilayer film with a 2-mil PVOH core layer and 2-mil PHA skin layers provided barrier properties better than each of the individual film components. OTR increased from 27 to 41 cc/m^2-day when the RH of the test was increased from 0 to 60% RH and to 52 cc/m^2-day at 90% RH. The PHA skin layers provided protection to the PVOH core layer from atmospheric moisture. It was also observed that the theoretical transmission rate calculated using the summation model did not properly estimate transmission of this film sample. When normalized to thickness, the core layer performed 91% better on a per-mil basis in the co-extruded structure than the monolayer structure. The normalized PVOH OTR value was determined by multiplying the PVOH OTR value at 0% RH (60 cc/m^2-day) by the thickness of the PVOH layer (4.9 mil) in that sample. This could indicate an increased level of orientation or crystallinity in the PVOH core layer in comparison with the film produced through monolayer processing as flow within a co-extruded structure is vastly different than flow in a monolayer structure. This theory was examined through DSC and mechanical analysis.

Because of the low peel strength of the layers in the structure, the core PVOH layer was separated from the PHA skin layers for analysis. DSC experiments showed that the amount of crystalline material in the monolayer PVOH film and monolayer PHA films was similar to that of their corresponding layers in the multilayer film. This result indicated that the enhanced level of oxygen barrier under dry conditions in the multilayer film was not due to an increased crystalline content of the PVOH or PHA layers in the multilayer film. Tensile testing of the monolayer PVOH and PHA as well as the core layer PVOH and PHA skin layers indicated clear differences between the materials. As illustrated in Figure 3, when tested in the machine direction, the PVOH core layer of the multilayer structure exhibited an average Young's Modulus that was roughly 83% greater than that of the monolayer PVOH film. Tensile strength at break was 38% greater in the core layer film than the monolayer film. Similar trends were observed in the PHA films. Young's modulus of the skin PHA layers was 260% greater than that of the monolayer PHA film and the tensile strength at break was 46% greater in the PHA skin.

These tensile property results indicate that the level of polymer chain orientation in the machine direction is greater in the core layer PVOH film and PHA skin layers than the monolayer PVOH and PHA films. Mono-axial chain orientation of polystyrene film has been shown to increase tensile strength by as much as 150% through stresses applied parallel to chain orientation.[32] Other experimentation has shown that the multilayer film extrusion process in flat films can produce highly oriented structures by extruding higher strength materials on either side of a weaker material, which will apply simultaneous stretching to both polymers.[33] Previous work on the effects of machine direction orientation on the gas barrier properties of polymers

Table II. Barrier Properties of Co-Extruded PHA–PVOH Film and Its Components

Sample	Gauge (mil)	OTR (cc/m^2-day) 0% RH	OTR (cc/m^2-day) 60% RH	OTR (cc/m^2-day) 90% RH	OPR (cc mil/m^2-day) 0% RH	OPR (cc mil/m^2-day) 60% RH	OPR (cc mil/m^2-day) 90% RH
POVAL PVOH	4.9	60	999	Fail	294	4924	Fail
PHA P2001	5.1	211	238	250	1076	1214	1275
PVOH-PHA multilayer (2-mil PVOH core) actual	6.8	27	41	52	N/A	N/A	N/A
PVOH-PHA multilayer (2-mil PVOH core) estimated	6.8	89	229	N/A	N/A	N/A	N/A

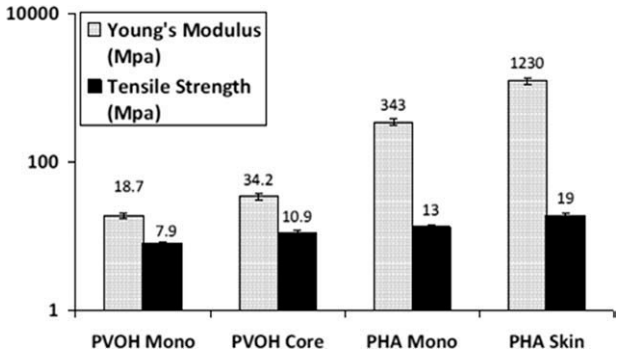

Figure 3. Tensile properties of monolayer PVOH and PHA films versus PVOH and PHA film layers from multilayer structure.

has been well-documented for polyethylene[33] and polypropylene.[34,35] Duckwall et al. clearly discusses this relationship with their work on high-density polyethylene films and how gas barrier properties were improved with higher degrees of chain orientation in the machine direction.[34] Tabatabaei et al. discuss the effects of orientation on the barrier properties of polypropylene films.[35] The improvement of gas barrier properties of EVOH and nylon through orientation of polymeric chains is also reported by Schut.[36] Although chain orientation appears to be an explanation for the enhanced properties observed, other factors are also contributing to these observations as this is a complex system involving a cast film process which does not typically impart high degrees of orientation. To investigate other phenomenon that could be affecting barrier and mechanical properties, DMA analysis was conducted on the films. Table III lists the results of the DMA testing before and after conditioning of the film samples as described in the experimental section.

Illustrated in Figure 4 is a representative DMA graph that shows the loss modulus, storage modulus, and tan delta of the PHA skin layer after conditioning. From Table III, the measured T_g of the PVOH is highly affected by moisture content. Water plasticizes PVOH and this trend is observed as the T_g is lower at higher moisture content. In the preconditioned films, the water content is lower in the core PVOH layer than the monolayer PVOH. This fact indicates that in the monolayer state, the PVOH film was more plasticized and will hence have a higher gas permeation rate and lower modulus as indicated by barrier testing and the mechanical properties analysis. Considering our results along with the reported results of the previously mentioned authors, it is possible that the PVOH core layer of our multilayer structure and the PHA skin layers had an increased level of chain orientation than the monolayer films. This helps explain the increased gas barrier properties of the multilayer film over the monolayer film and the differences between the theoretical and actual higher measured permeation values. Decreased plasticization of the PVOH core layer due to lower moisture content (confirmed through moisture analysis) has also improved the barrier properties of the multilayer film and has increased the modulus of the film. It appears that the moisture content of the PHA skin layers had less of an effect on the barrier and mechanical properties than the orientation of the PHA polymer chains.

Although the processing of the film appeared to be quite successful, the resistance of the film to delamination was quite low (0.004 N/mm) and needed to be increased to obtain a functional film. The PEG plasticizer in the PVOH core layer may be a cause for the reduced adhesion between polymer layers. The use of plasticized materials in multilayer structures often increases delamination and reduces the peel strength of the layers in the system significantly. Martin et al. report that the use of 20% PEG in a multilayer polyester-based system decreased the peel strength of the layers from 0.05 to 0.02 N/mm.[37] Graziano and Sjostrand report how the migration of plasticizers from flexible polyvinyl chloride films to polymeric coatings limits the use of many pressure sensitive adhesives to nonvinyl applications.[38] Biodegradable compositions based on thermoplastic starch, a plasticized starch, are also affected by plasticizer leaching and materials compatibility.[39] Table III indicates that the T_g of the PVOH monolayer, as measured by DMA, is 10°C lower than the PVOH layer in the multilayer film. This shift indicates that PEG plasticizer and water are most likely present at the surface of the PVOH film in the structure. This will play a large role in causing delamination of the layers once in a multilayer system. Numerous methods of improving adhesion between polymer layers may be considered. These methods include increasing the land length of the film die, reactive extrusion, and increased wetting of the polymers.

Reactive extrusion processing was investigated to provide a means for the hydroxyl groups of the PVOH structure to bond

Table III. DMA Analysis of Monolayer Films and Delaminated Film Layers

Sample	Initial moisture content (%)	T_g (°C)	Final moisture content (%)	T_g (°C)
PHA monolayer	0.23	0.8	0.22	2.1
PHA skin layer	0.26	5.1	0.21	1.4
PVOH monolayer	2.59	−1.5	1.73	13.5
PVOH core layer	2.07	1.6	1.44	8.5

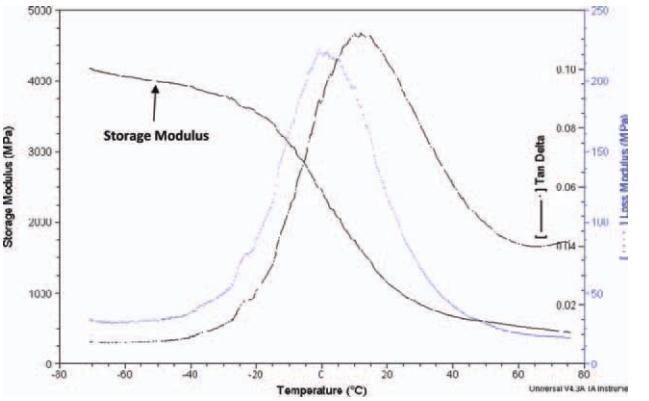

Figure 4. Representative DMA curves for PHA skin layer analysis. [Color figure can be viewed in the online issue, which is available at wileyonlinelibrary.com.]

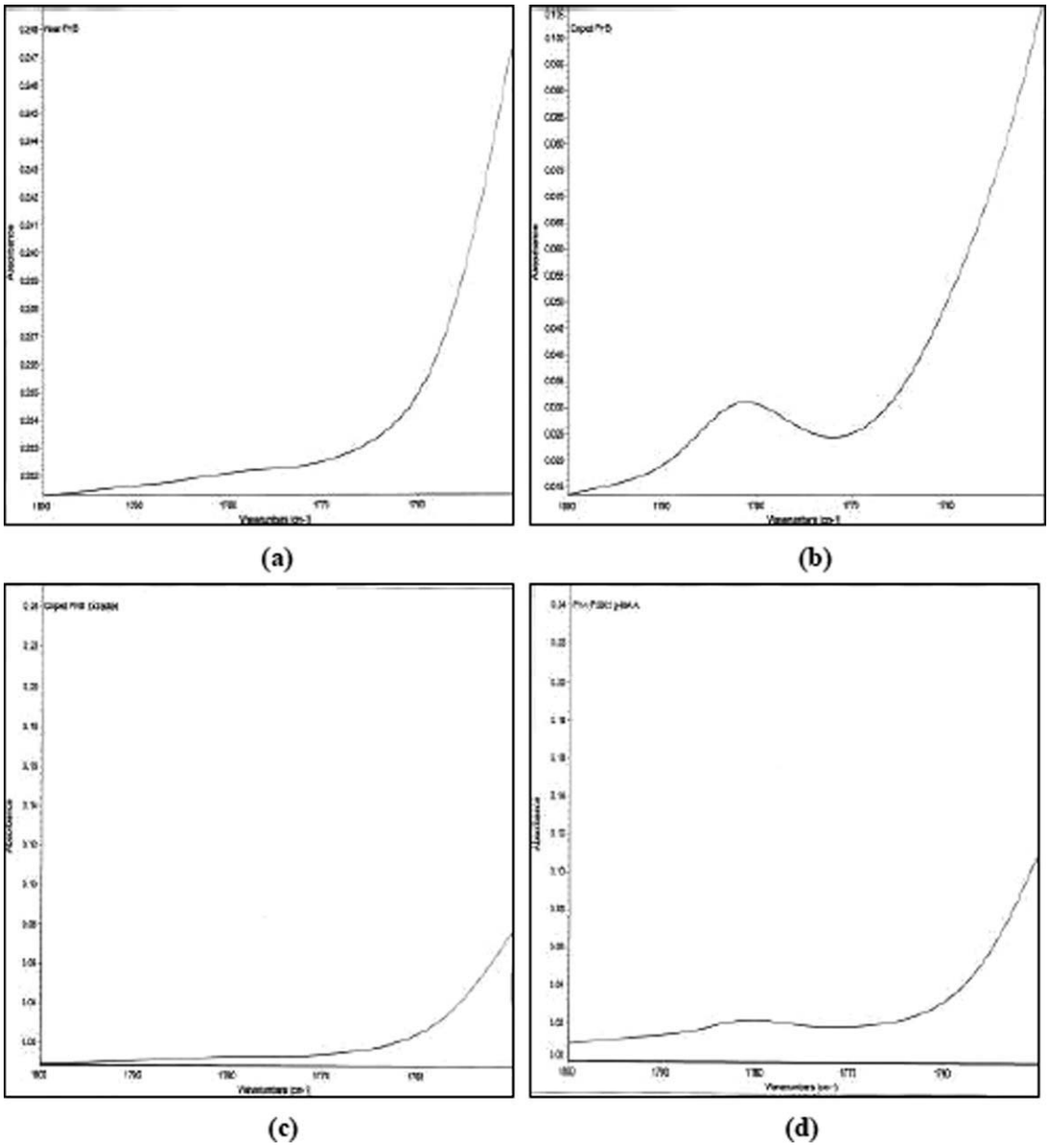

Figure 5. FTIR spectra for (a) neat PHB polymer after extrusion, (b) PHB doped with maleic anhydride without peroxide initiator, (c) doped PHB after purification, and (d) PHB-*g*-MA sample after purification.

with maleic anhydride grafted onto the PHA, thereby increasing adhesion strength and peel resistance. A reactive extrusion method for grafting maleic anhydride onto a PHB polymeric chain has been described by Mohanty et al. to enhance interfacial adhesion between natural fibers and the PHB matrix in a PHB/fiber blend.[40]

Maleic anhydride-grafted PHA was formulated according to the procedure outlined previously and characterized to confirm the occurrence of the grafting reaction. Figure 5 (a) illustrates the FTIR absorbance spectra in the range of interest (1800–1750 cm^{-1}) of neat PHA after extrusion, and Figure 5(b) illustrates the spectra in the same range of a PHA sample with maleic anhydride added in the absence of the peroxide initiator.

In Figure 5(a), the dominant peak in the spectra begins at 1719 cm^{-1}, and represents the carbonyl (C[dbons]O) band of the polyester group. A new peak is observed in Figure 5(b) at 1780 cm^{-1}, which arises from the presence of the anhydride group in the sample. Figure 5(c) shows data for the same sample following solvent-extraction of the maleic anhydride; the peak present in Figure 5(b) is not observed in Figure 5(c), indicating complete removal. Figure 5(d) illustrates that FTIR spectra obtained for the grafted PHA-*g*-MA sample. This sample was purified through the same solvent-extraction procedure as the sample in Figure 5(c). In this case, the peak at 1780 cm^{-1} remains which indicates that the purification technique did not remove all of the maleic anhydride from the sample. This is consistent with successful grafting of the PHA with maleic anhydride. To

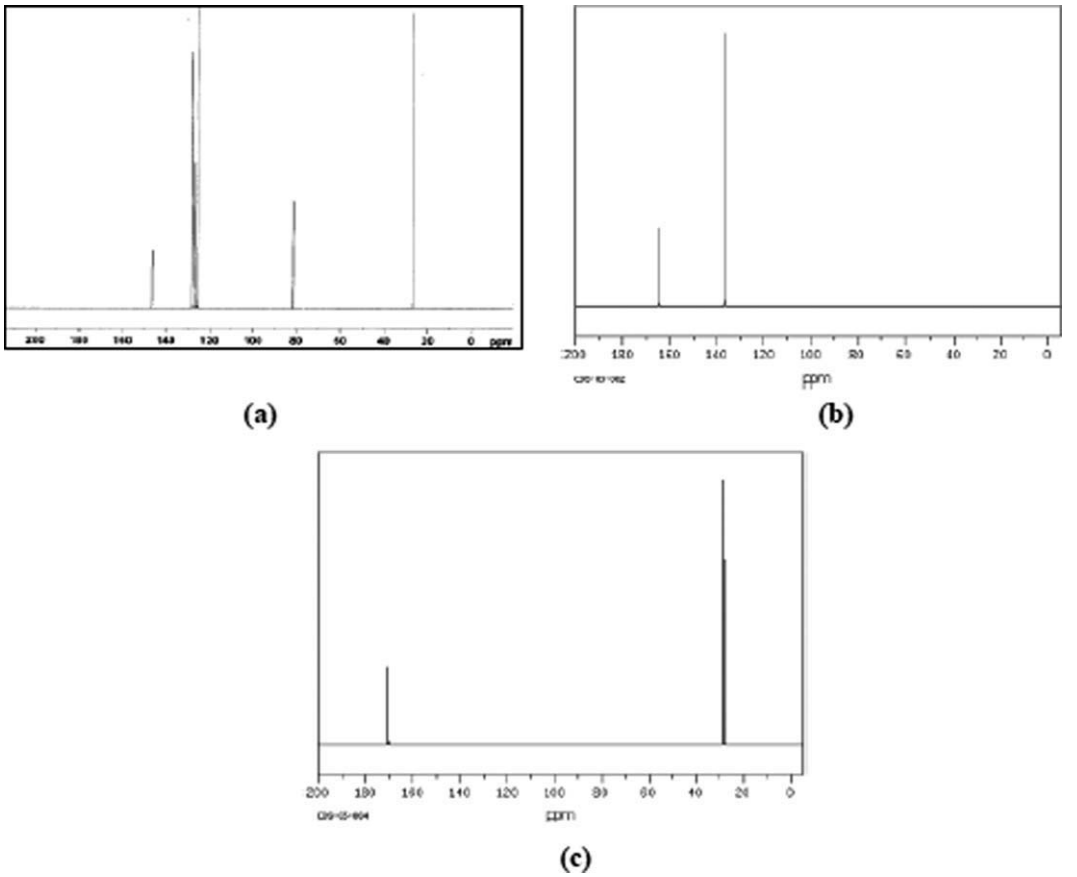

Figure 6. ^{13}C-NMR spectrum for (a) dicumyl peroxide, (b) maleic anhydride, and (c) succinic anhydride.

confirm this result, ^{13}C-NMR analysis was conducted on the samples.

Presented in Figure 6 are control ^{13}C-NMR spectra for dicumyl peroxide, maleic anhydride, and succinic anhydride for spectral comparison purposes.[41] The latter is included as a reference because the grafting reaction is expected to result in a loss of the double bond in the maleic anhydride ring. Figure 7 shows ^{13}C-NMR spectra (0–100 ppm) for neat PHA and PHA-*g*-MA samples that were purified via solvent-extraction with ethanol and chloroform. Figure 8 shows the spectra of the same samples in the 100–220 ppm range. Note that the large peaks from 76.7–77.8 ppm are due to the chloroform NMR solvent and are not associated with the sample. Examining the spectra, a peak appears in the PHA-*g*-MA sample at 26.9 ppm that is weak in the neat sample. This peak is likely due to the presence of a small amount of unreacted peroxide remaining in the sample. A scan of pure dicumyl peroxide (Figure 6) shows this peak at 26.9 ppm. Another interesting peak in this area is located at 29.4 ppm in the PHA-*g*-MA sample, but is weak or missing from the neat PHA sample. This is consistent with the presence of a grafted maleic anhydride group. As noted previously, when maleic anhydride is grafted to a polymer, it loses its double bond and the NMR spectra should be more like that of succinic anhydride. The NMR spectrum of pure succinic anhydride indicates a peak at 28.4 ppm. The new peak observed in this sample at 29.4 ppm is very similar to those observed for a succinic anhydride system, with a small shift that could be due to the bonding with the PHA chain. Additional differences in the PHA-*g*-MA spectrum are observed at 43.7 ppm, 73.0 ppm, between 120 and 135 ppm, at 137 ppm and 166.5 ppm. The peak at 43.7 ppm is assigned to the methine (CH) group of the grafted MA ring, whereaas the 73.0 ppm peak is assigned to the methine (CH) associated with the P3HB methyl branch. The small peaks present between 120 and 135 ppm are most likely related to the presence of residual dicumyl peroxide or its decomposition products. Finally, the peak at 137 ppm corresponds to the methine (CH) groups in the ungrafted maleic anhydride, whereas the peak at 166.5 ppm is assigned to the carbonyl carbon of the ungrafted maleic anhydride. In comparison, the grafted MA carbonyl carbon, which would be expected at 170.6 ppm based on the succinic anhydride spectrum, is obscured by peaks from the PHA. Chen et al. reported similar peaks in their maleated PHB samples and indicate that these are likely from single succinic anhydride rings that are formed when MA reacts with a tertiary radical site on the PHB backbone.[42] Many peaks presented in the spectra of Figures 7 and 8 closely resemble those found in other published work on maleic anhydride grafted PHAs.[43] A summary of the peaks observed in the ^{13}C-NMR spectrum of PHA-*g*-MA but not neat PHA are listed in Table IV, as well as proposed peak assignments. Although the presence of some ungrafted and degraded material cannot be entirely ruled out, this combined FTIR and ^{13}C-NMR

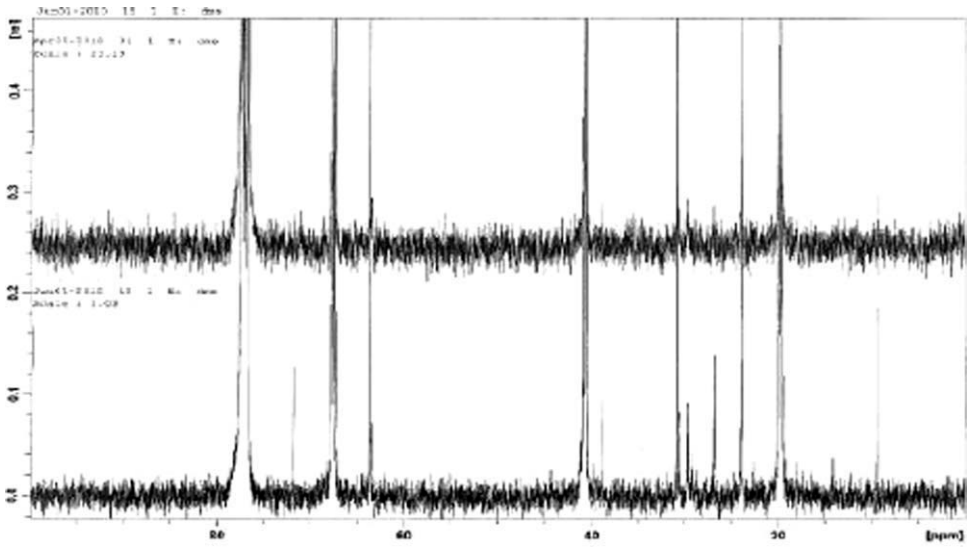

Figure 7. ^{13}C-NMR spectra for neat PHB (top) and purified PHB-*g*-MA (bottom) in the range of 0–100 ppm.

analysis strongly supports the conclusion that the desired grafting reaction has occurred.

Additional confirmation of the grafting reaction lies in the improvement of adhesion between the PHB and PVOH polymer layers. The results of the multilayer film peel tests are presented in Table V. This data indicates that with the incorporation of the PHA-*g*-MA polymer as a tie layer, the peel strength between PVOH and PHB layers are increased in the multilayer film structure. The measured average force increased by greater than 2× from 0.15 to 0.34 N/mm, and the stress increased by greater than 5× from 682 to 3484 kPa. This improvement in average force and stress indicates greater peel strength between the polymer layers. This is a direct result of the improved adhesion properties between the polymers due to the bonding of the grafted anhydride to the hydroxyl groups of the PVOH polymer in the multilayer system as this bonding improvement is not observed without the PHA-*g*-MA component. Unfortunately, permeation testing was not possible on the PHB-*g*-MA multilayer samples as only a small quantity of grafted material was produced. Proper multilayer film trials will require the production of significantly more grafted resin that is optimized for grafting efficiency and level.

The results of the biodegradation testing, according to ASTM 6691, are presented in Figure 9. In this figure, the average percent mineralization (biodegradation) for the triplicate samples is presented for the neat PHA, the maleic anhydride grafted PHA (PHA-*g*-MA), the PVOH, and a Kraft paper control as a function of time.

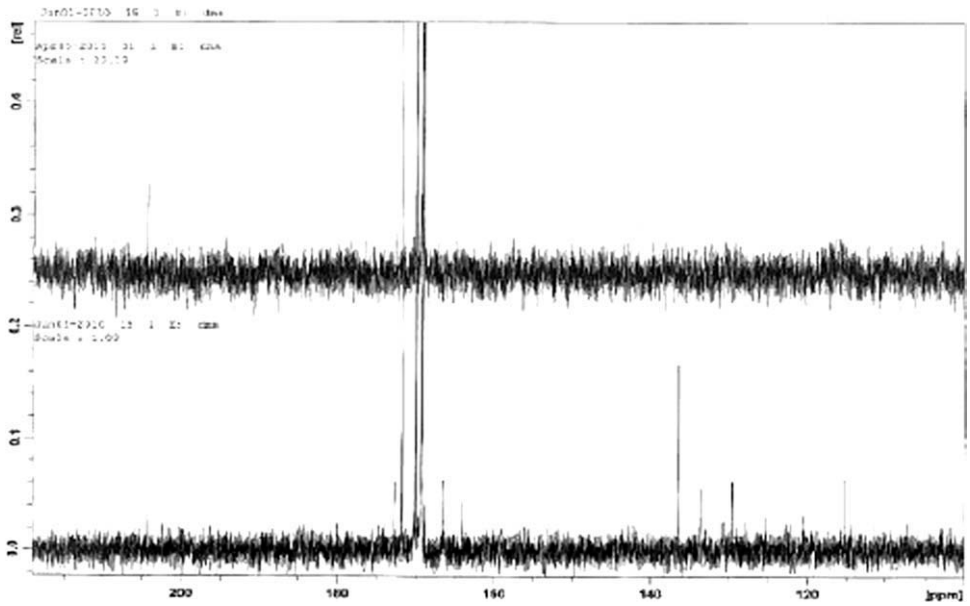

Figure 8. ^{13}C-NMR spectra for neat PHB (top) and purified PHB-*g*-MA (bottom) in the range of 100–220 ppm.

Table IV. Summary of ^{13}C-NMR Peak Shifts

Peak location (ppm)	Assignment	Description
26.9	Dicumyl peroxide	Residual unreacted dicumyl peroxide
28.4–29.4	Grafted MA CH_2	Maleic anhydride following grafting to PHA (double bond converted to single)
43.7	Grafted MA CH	Maleic anhydride following grafting to PHA (double bond converted to single)
73.0	Grafted P3HB CH	P3HB methine following MA grafting
76.7–77.8	Chloroform	NMR solvent
120.0–135.0	Aromatic ring carbons	Dicumyl peroxide or its decomposition products

Figure 9 indicates that both the PHA P2001 and the maleic anhydride grafted PHA P2001 polymer samples displayed high rates of biodegradation according to ASTM D6691, along with the Kraft paper control. After 90 days of incubation, the ungrafted sample had reached 97% mineralization. The maleic-anhydride grafted sample reached 84% mineralization in the same time frame. These initial tests indicate that small differences have been observed in the mineralization rates and curve shapes between the ungrafted and grafted samples. The grafted maleic anhydride appears to slow down the mineralization rate slightly at the beginning of the test, causing lower overall biodegradation than the ungrafted sample after 90 days of incubation. During the same test, the PVOH sample displays a very low rate of mineralization and reaches just above 12% mineralization during the same time period. Although the PVOH is completely dissolved, the conversion of carbon to carbon dioxide is occurring very slowly in comparison with the PHA and Kraft paper samples.

CONCLUSIONS

Multilayer films consisting of a melt-extrudable PVOH core and PHA skin layers were successfully produced through the co-extrusion process on a laboratory-scale extrusion line. Gas barrier testing of the multilayer films indicated that the OTR of the multilayer film with a 2-mil PVOH core layer and 2-mil PHA skin layers increased from 27 to 41 cc/m^2-day when the RH of the test was increased from 0 to 60% RH and to 52 cc/m^2-day at 90% RH. It is evident that relative humidity significantly affects barrier properties in this film, but the PHA skin layer does provide some level of protection to the water-soluble PVOH core. Enhanced barrier properties may be achievable through the use of a less plasticized PVOH grade and a higher crystallinity grade of PHA. The data gathered from thermal and mechanical analysis of the samples is evidence that polymers behave differently in a multilayer structure than when in a monolayer film. Crystallinity and chain orientation can be altered during the multilayer process, which will ultimately determine the final properties of the structure. As with most hydroscopic polymers, moisture content varied between the monolayer and multilayer films. This moisture had a significant plasticization affect on the polymers in the system, altering the T_g of the polymers and therefore changing mechanical and barrier properties. It appears that a combination of increased polymer chain orientation and decreased plasticization in the multilayer film caused the improvements observed in the layers of the multilayer system over the monolayer films.

FTIR and NMR characterization methods have indicated that a maleic anhydride grafted PHB polymer was successfully produced through a reactive extrusion technique using a dicumyl peroxide initiator. The grafted PHA polymer directly improved the adhesion of the PVOH layer to the PHB layer in the multilayer films by acting as a tie layer between the two polymers in the structure. This improvement in adhesion strength, although modest, is encouraging in the development of a bio-based and biodegradable tie layer resin for multilayer biopolymer films.

Finally, biodegradation experiments according to ASTM D6691 indicate small differences in the rate and shape of the mineralization curves when comparing the grafted and ungrafted PHA samples. It appears that the addition of the maleic anhydride to the PHA polymer chain hinders the microbial attack slightly, thereby slowing down biodegradation rates slightly. Further testing with PHA samples grafted at various degrees would support this theory. Comparison of a PVOH sample to the PHA indicates that mineralization of PVOH occurs at levels much lower than the PHA and glucose controls even though it is completely dissolved in the natural seawater.

Table V. Results of Peel Testing for Multilayer Films

Sample	Average force (N/mm)	Average stress (kPa)
PHB/PVOH	0.15 ± 0.05	682 ± 296
PHB/PHB-*g*-MA/PVOH	0.34 ± 0.05	3484 ± 1331

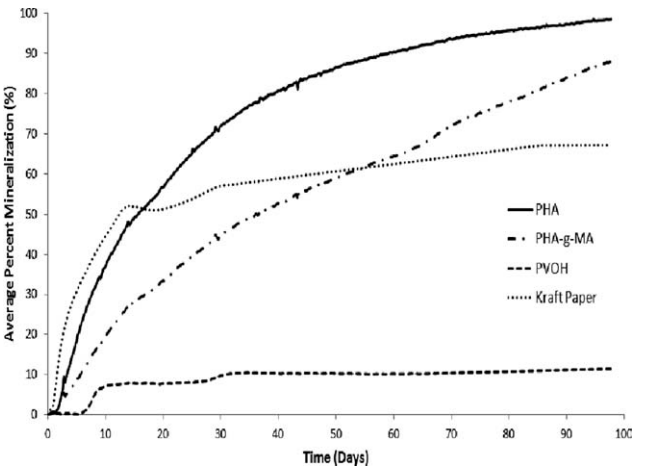

Figure 9. Average percent mineralization of the samples in natural seawater according to ASTM D6691.

ACKNOWLEDGMENTS

The authors thank the U.S. Navy Waste Reduction Afloat Protects the Sea (WRAPS) program, especially Mr. Jeff Whitman, Mr. John Bendick, and Mr. Trey Kunkel, for funding the research discussed in this article. A special acknowledgement goes to Dr. Robert Whitehouse of Metabolix Inc., Professor Daniel Schmidt, and Professor Stephen McCarthy of the University of Massachusetts Lowell for working with the NSRDEC on this project and supplying their knowledge and expertise in the area of PHA polymers. Heather Scaglione of A. Schulman, Ken Kumaki of Kuraray, and Terrence Cooper are also acknowledged for providing PVOH sample materials along with their experience in the area of PVOH films and processing. They also thank Dr. Joel Carlson and Ms. Diane Steeves for their FTIR and NMR expertise, as well as Ms. Danielle Froio, Mr. Matthew Bernasconi, Mr. Christopher Hope, and Ms. Jeanne Lucciarini of the NSRDEC for all of their efforts in relation to this research. This research could not have been accomplished without their efforts.

REFERENCES

1. Mohan, A. M. *Packag. Dig.* **2005,** *42,* 50.
2. Maiti, P.; Batt, C.; Giannelis, E. Biomacromolecules **2007,** *8,* 3393.
3. Ratto, J.; Thellen, C.; Lucciarini, J. In Industry Guide to Polymer Nanocomposites; Beyer, G., Ed.; Plastics Information Direct: United Kingdom, **2009.**
4. Sanchez-Garcia, M. D.; Gimenez, E.; Lagaron, J. M. *J. Appl. Polym. Sci.* **2008,** *108,* 2787.
5. Reguera, J.; Lagaron, J. M.; Alonso, M.; Reboto, V.; Calvo, B.; Rodriguez-Cabello, J. C. *Macromolecules* **2003,** *36,* 8470.
6. Tang, X.; Alavi, S. *Carbohydr. Polym.* **2011,** *85,* 7.
7. Chiellini, E.; Corti, A.; D'Antone, S.; Solaro, R. *Prog. Polym. Sci.* **2003,** *28,* 963.
8. Consortium für Elektrochemishe Industrie Gmbh. Ger. Pat. 450,286 (**1924).**
9. Consortium für Elektrochemishe Industrie Gmbh. Can. Pat. 265,172 (**1926).**
10. Cooper, T.; Harrison, P.; Wilkes, T. In Proceedings of the 8th Annual Global Plastics Environmental Conference (GPEC); Society of Plastics Engineers: Detroit, **2002;** p 360.
11. Jack, R. L. (to British Technology Group). U.K. Pat. GB 2,291,831B (**1997).**
12. Jack, R. L. (to British Technology Group). U.S. Pat. 6,080,346 (**2000).**
13. Stevens, H.G.; Dawson, J. C. (Pvaxx Technologies Ltd.). Int. Pat. WO 64,421 (**2001).**
14. Doi, Y. Microbial Polyesters; VCH Publishers: New York, **1990.**
15. Thellen, C.; Coyne, M.; Froio, D.; Auerbach, M.; Wirsen, C.; Ratto, J. *J. Polym. Environ.* **2008,** *16,* 1.
16. LaTuga, B.; Ramirez, S.; Arceo, J.; Flythe, M.; Rowe, S.; Baron, S.; Dennis, D.; Augustine, B. *Polym. Mater. Sci. Eng.* **2003,** *88,* 277.
17. Jendrossek D.; Schirmer, A.; Schlegel, H. *Appl. Microbiol. Biotechnol.* **1996,** *46,* 451.
18. Doi, Y.; Kanesawa, Y.; Tanahashi, N.; Kumagal, Y. *Polym. Degrad. Stab.* **1992,** *36,* 173.
19. Madison, L.; Huisman, G. *Microbiol. Mol. Biol. Rev.* **1999,** *63,* 21.
20. Sridewi, N.; Bhubalan, K.; Sudesh, K. *Polym. Degrad. Stab.* **2006,** *91,* 2931.
21. Song, C.; Wang, S.; Ono, S.; Zhang, B.; Shimasaki, C.; Inoue, M. *Polym. Adv. Technol.* **2003,** *14,* 184.
22. Gao, H.; Chen, J.; Du, G.; Wu, Y.; Lun, S. *Zhongguo Huanjing Kexue* **1997,** *17,* 330.
23. Ho, Y.-H.; Gan, S.-N.; Tan, I. *Appl. Biochem. Biotechnol.* **2002,** *102,* 337.
24. Ratto, J.; Russo, J.; Allen, A.; Herbert, J.; Wirsen, C. *ACS Symp. Ser.* **2001,** *786,* 316.
25. Graff, G.; Williford, E.; Burrows, P. *J. Appl. Phys.* **2004,** *96,* 1840.
26. Vargas, E.; Butler, T.; Veazey, E. TAPPI Film Extrusion Manual: Process, Materials, and Properties; TAPPI Press: Atlanta, GA, **1992;** pp 44–47.
27. Mount, E. M. Co-Extrusion Principles and Practices Seminar; Society of Plastics Engineers: Brookfield, CT, **2005;** pp 22–23.
28. Metabolix Incorporated Website. Available at: http://www.metabolix.com. Accessed on October 30, **2007.**
29. Arkema Peroxide Half-Life Selection Guide. Available at: www.arkema-inc.com. Accessed on January 6, **2010.**
30. Mount, E.; Giles, H.; Wagner, J. Extrusion: The Definitive Processing Guide and Handbook; William Andrews Incorporated, Norwich, NY, USA, **2005.**
31. Firdaus, V.; Tong, P. P. *J. Plast. Film Sheeting* **1992,** *8,* 333.
32. Deanin, R. Polymer Structure, Properties and Applications; Cahners Publishing: Boston, **1972.**
33. Takashige, M.; Kanai, T. Film Processing; Hanser/Gardner Publications: Cincinnati, **1999.**
34. Duckwall, L. R.; Bastian, D. H.; Hatfield, E. U.S. Pat. 6,394,411 (**2002).**
35. Tabatabaei, S. H.; Carreau, P. J.; Ajji, A. *Polymer* **2009,** *50,* 3981.
36. Schut, J. H. *Plast. Technol.* **2005,** *51,* 48.
37. Martin, O.; Schwach, E.; Averous, L.; Couturier, Y. *Starch* **2001,** *53,* 372.
38. Graziano, L.; Sjostrand, S. *J. Plast. Film Sheeting* **1986,** *2,* 95.
39. Averous, L. *Polym. Rev.* **2004,** *44,* 231.
40. Mohanty, A.; Drzal, L.; Mulukutla, P.; Desai, S.; Misra, M. In Proceedings of the Society of Plastics Engineers Annual Technical Conference (ANTEC), Chicago, IL, **2004;** pp 1483–1487.
41. SDBSWeb (National Institute of Advanced Industrial Science and Technology). Available at: http://riodb01.ibase.aist.go.jp/sdbs/. Accessed on August 12, **2010.**
42. Chen, C.; Peng, S.; Fei, B.; Zhuang, Y.; Dong, L.; Feng, Z.; Chen, S.; Xia, H. *J. Appl. Polym. Sci.* **2003,** *88,* 659.
43. Hong, S.; Lin, Y.; Lin, C. *J. Appl. Polym. Sci.* **2008,** *110,* 2718.